AGU PUBLICATIONS

Geophysical Research Letters

RESEARCH LETTER
10.1002/2015GL067398

Key Points:
- Distributions of ULF PSD under different geomagnetic activities are studied
- Electric radial diffusion coefficients of radiation belt electrons are calculated
- Differences between our results and previous D_{LL} models are discussed

Correspondence to:
W. Liu,
liuwenlong@buaa.edu.cn

Citation:
Liu, W., W. Tu, X. Li, T. Sarris, Y. Khotyaintsev, H. Fu, H. Zhang, and Q. Shi (2016), On the calculation of electric diffusion coefficient of radiation belt electrons with in situ electric field measurements by THEMIS, *Geophys. Res. Lett.*, *43*, 1023–1030, doi:10.1002/2015GL067398.

Received 14 DEC 2015
Accepted 20 JAN 2016
Accepted article online 22 JAN 2016
Published online 13 FEB 2016

On the calculation of electric diffusion coefficient of radiation belt electrons with in situ electric field measurements by THEMIS

Wenlong Liu[1], Weichao Tu[2], Xinlin Li[3], Theodore Sarris[3,4], Yuri Khotyaintsev[5], Huishan Fu[1], Hui Zhang[6], and Quanqi Shi[7]

[1]School of Space and Environment, Beihang University, Beijing, China, [2]Department of Physics and Astronomy, West Virginia University, Morgantown, West Virginia, USA, [3]Laboratory for Atmospheric and Space Physics, University of Colorado at Boulder, Boulder, Colorado, USA, [4]Space Research Laboratory, Democritus University, Xanthi, Greece, [5]Swedish Institute of Space Physics, Uppsala, Sweden, [6]Institute of Geology and Geophysics, Chinese Academy of Sciences, Beijing, China, [7]School of Space Science and Physics, Shandong University, Weihai, China

Abstract Based on 7 years' observations from Time History of Events and Macroscale Interactions during Substorms (THEMIS), we investigate the statistical distribution of electric field Pc5 ULF wave power under different geomagnetic activities and calculate the radial diffusion coefficient due to electric field, D_{LL}^{E}, for outer radiation belt electrons. A simple empirical expression of D_{LL}^{E}[THEMIS] is also derived. Subsequently, we compare D_{LL}^{E}[THEMIS] to previous D_{LL} models and find similar *Kp* dependence with the D_{LL}^{E}[CRRES] model, which is also based on in situ electric field measurements. The absolute value of D_{LL}^{E}[THEMIS] is constantly higher than D_{LL}^{E}[CRRES], probably due to the limited orbital coverage of CRRES. The differences between D_{LL}^{E}[THEMIS] and the commonly used D_{LL}^{M}[B-A] and D_{LL}^{E}[Ozeke] models are significant, especially in *Kp* dependence and energy dependence. Possible reasons for these differences and their implications are discussed. The diffusion coefficient provided in this paper, which also has energy dependence, will be an important contributor to quantify the radial diffusion process of radiation belt electrons.

1. Introduction

In the Earth's radiation belt, ~MeV electrons are trapped by the Earth's magnetic field to interact with various types of electromagnetic waves [e.g., *Li et al*., 2005; *Xiao et al*., 2009; *Thorne*, 2010; *Su et al*., 2011]. One of the fundamental interactions between electrons and electromagnetic waves is the drift resonance that causes electrons to diffuse inward and outward [e.g., *Fu et al*., 2011], depending on the radial gradient of the phase space density. This process is known as radial diffusion [e.g., *Schulz and Lanzerotti*, 1974]. Radial diffusion requires electromagnetic waves in a frequency range that is comparable to the drift frequency of relativistic electrons around the Earth, which is usually several millihertz and roughly corresponds to the Pc5 (2 to 6.7 mHz) and Pc4 (6.7 to 22 mHz) frequency of ultralow frequency (ULF) waves.

The radial diffusion coefficient (D_{LL}) is a key parameter in quantifying the efficiency of radial diffusion. Early studies [e.g., *Fälthammar*, 1965; *Brautigam and Albert*, 2000] calculated D_{LL} as the sum of electromagnetic $\left(D_{LL}^{M}\right)$ and electrostatic $\left(D_{LL}^{E_{\text{static}}}\right)$ diffusion coefficient. However, because it is difficult to separate the inductive term from the convective term in electric field measurements, efforts have been made to combine electromagnetic and electrostatic diffusion coefficient together as electric diffusion coefficient $\left(D_{LL}^{E}\right)$, leaving the rest of D_{LL} as the diffusion coefficient due to compressional magnetic field $\left(D_{LL}^{B}\right)$. For example, *Fei et al*. [2006] theoretically derived equations to calculate D_{LL} using measurements of electric field and magnetic field wave power as

$$\begin{aligned} D_{LL}^{E} &= \frac{L^6}{8R_E^2 B_E^2}\sum_m P_m^E(m\omega_d) \\ D_{LL}^{B} &= \frac{\mu^2 L^4}{8q^2\gamma^2 R_E^4 B_E^2}\sum_m m^2 P_m^B(m\omega_d) \\ D_{LL}^{\text{total}} &= D_{LL}^{E} + D_{LL}^{B} \end{aligned} \tag{1}$$

where m is the azimuthal wave number, ω_d is the drift frequency, P is the power spectral density (PSD) as function of frequency, μ is the magnetic moment (or the first adiabatic invariant of electrons), and γ is the

relativistic factor. The constants B_E, R_E, and q are the equatorial magnetic field strength at the surface of the Earth, the Earth's radius, and the electron charge, respectively. These equations have been widely used to calculate D_{LL} with ULF wave PSD obtained from observations [*Ozeke et al*., 2012, 2014; *Ali et al*., 2015] and MHD simulations [*Huang et al*., 2010; *Tu et al*., 2012]. However, in the derivation of *Fei et al*. [2006], they assume no phase relation between the electric and magnetic field perturbations, introducing uncertainties that have not been well quantified yet [*Lejosne et al*., 2013].

Several models of D_{LL} have been developed and have been used in radiation belt simulations to solve the Fokker-Plank equation. One of them is the *Brautigam and Albert* [2000] model (known as D_{LL}^{M}[B-A]), which is established based on empirical formulae and limited point measurements. *Brautigam et al*. [2005] used in situ CRRES electric field measurements to calculate D_{LL}^{E} (known as D_{LL}^{E}[CRRES]). However, assumptions have been made because CRRES could only provide electric field measurements in the y and z components in GSM coordinate system and its orbit does not have complete local time coverage. More recently, *Ozeke et al*. [2012] used 15 years of ground magnetometer observations to infer the electric ULF wave power in space and developed a model to calculate D_{LL}^{E}. Later, *Ozeke et al*. [2014] established an analytic model for D_{LL}^{E} and D_{LL}^{B} (known as D_{LL}^{E}[Ozeke] and D_{LL}^{B}[Ozeke], respectively). *Ali et al*. [2015] used magnetic field measurements from CRRES to calculate magnetic ULF wave power and estimated D_{LL}^{B} (known as D_{LL}^{B}[CRRES]). These recent studies suggested that the radial diffusion is mostly controlled by electric ULF wave with D_{LL}^{E} greater than D_{LL}^{B} by orders of magnitude.

The accuracy of D_{LL}^{E} estimation relies on the understanding of ULF waves in the inner magnetosphere. The ULF waves are abundant in the inner magnetosphere generated by external sources like the disturbance in the solar wind [*Leonovich et al*., 2003; *Mcpherron*, 2005] and internal sources like instabilities and the braking of the earthward high-speed flow in the plasma sheet [*Kepko and Kivelson*, 1999; *Lu et al*., 2002; *Cao et al*., 2008, 2010; *Yeoman et al*., 2012; *Dai et al*., 2013; *Klimushkin and Mager*, 2015; *Zhou et al*., 2015]. With recent improvement on in situ electric field measurements by THEMIS [*Angelopoulos*, 2008] and Van Allen Probes, ULF wave distributions have been further studied [*Liu et al*., 2009; *Takahashi et al*., 2015a, 2015b; *Dai et al*., 2015]. Especially, several studies [*Sarris et al*., 2009; *Hartinger et al*., 2011; *Liu et al*., 2013] demonstrate that THEMIS measurements are able to provide accurate electric field of the ULF waves in the two components near the equatorial plane, hence providing the critical information to calculate azimuthal electric field ULF wave power. *Liu et al*. [2009] studied the statistical distribution of ULF wave power with 1 year of observations; however, the data volume in that paper was not adequate to build a D_{LL}^{E} model. In this study, we will use long-term in situ electric field measurements by the THEMIS mission to study the statistical distributions of electric ULF wave power and subsequently, we calculate the electric radial diffusion coefficient. The calculated D_{LL}^{E} will be compared with other D_{LL} models.

2. Observation of the PSD of E_φ

Electric field measurements from the electric field instrument (EFI) [*Bonnell et al*., 2008] on board THEMIS-D from January 2008 to December 2014 are used to calculate the power spectral density (PSD) of ULF waves. The measurements are transformed into the mean field-aligned coordinate system [e.g., *Takahashi et al*., 2015a, 2015b]. In this system, $B_{//}$ is obtained from a 60 min running average of the magnetic field, centered at the data point that is being processed. The azimuthal direction $\hat{e}_\varphi$ is determined by $\hat{e}_{//} \times \frac{\vec{r}}{E}$, where $\hat{e}_{//}$ points along the average background magnetic field and $\frac{\vec{r}}{E}$ is the radial position vector, pointing outward. The radial direction $\hat{e}_r$ completes the orthogonal system ($\hat{e}_r$, $\hat{e}_\varphi$, and $\hat{e}_{//}$). The PSDs are calculated by a Morlet wavelet technique [*Morlet et al*., 1982] with a Hanning window performed on spin-averaged (~3 s) electric field data. Subsequently, the obtained 3 s PSDs are averaged in 5 min windows. Each 5 min averaged PSD value is considered as one sample in this study. The integrated PSDs in Pc3 to Pc5 frequency bands are processed and stored at the Maarble Project website (http://www.maarble.eu/) available for the community.

The data samples are first divided into six categories of geomagnetic conditions based on the values of *Kp* index, as $Kp = 0$ for 0, 0+ values, $Kp = 1$ for 1−, 1, 1+ values, etc. We select the data samples with magnetic latitudes within 15° from the magnetic equator, in order to decrease the effect of the latitudinal distribution

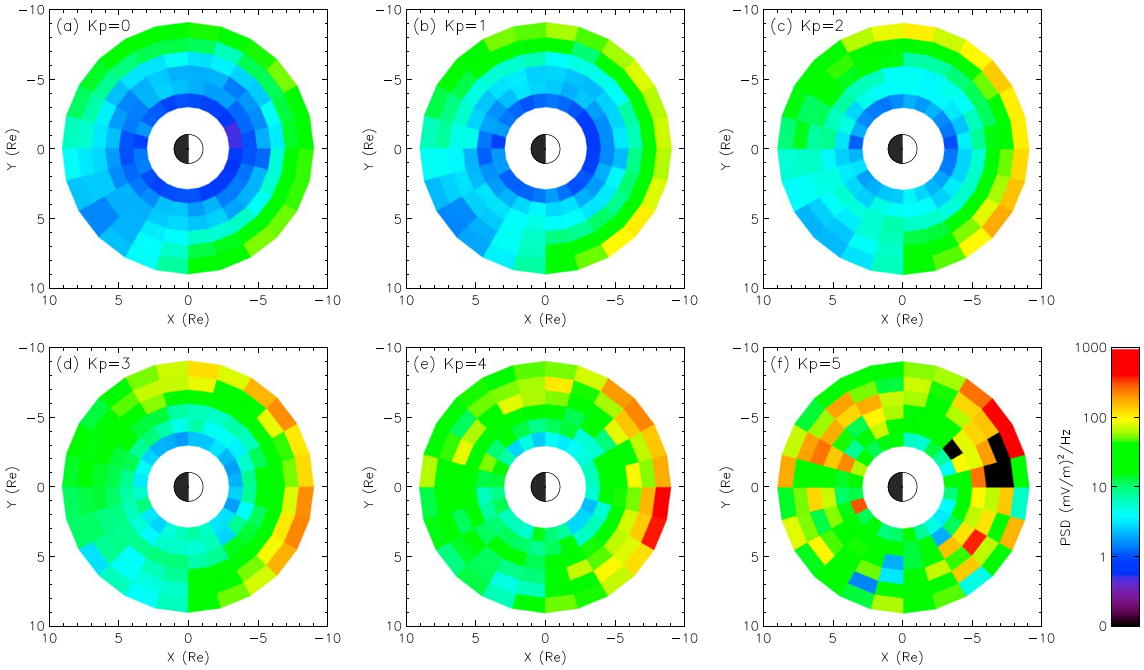

Figure 1. Distributions of Pc5 ULF wave power in the E_φ component in the equatorial plane based on 7 years, January 2008 to December 2014, observations of THEMIS for *Kp* levels (a–f) from 0 to 5.

of ULF waves. The data samples are then binned in spatial pixels for 24 MLT sectors and from $L = 3$ to 8 with 1 R_E step labeled as $L = 3.5$ to 7.5, respectively. The integrated PSDs of azimuthal electric field (E_φ) over Pc5 frequency range are collected for each spatial pixel, and their median values in each pixel are subsequently calculated and plotted in Figure 1. Figures 1a to 1f represent the distributions of $Kp = 0$ to 5, respectively.

It is clearly shown in Figure 1 that larger PSD is observed in high *L* region than in low *L* region, which is consistent with the interpretation that the energy of Pc5 ULF wave is mainly supplied from external sources, from the solar wind [*Liu et al.*, 2009, 2010]. The wave power is stronger in the dayside than in the nightside and shows an asymmetry in the nightside with more power in the premidnight sector than in the postmidnight sector. As the geomagnetic activity enhances, the PSD of E_φ increased as shown from Figures 1a–1f by about 1 order of magnitude as *Kp* increases from 0 to 5. It can also be seen that ULF wave power penetrates deeper into the inner region (smaller *L*) as the *Kp* index increases.

3. Calculation of D_{LL}^E

In order to calculate D_{LL}^E, we need the averaged E_φ PSD experienced by an electron during one drift orbit. With the assumption of dipole magnetic field model, the drift-averaged PSD can be obtained by calculating the median value of PSDs of all the data samples observed at each designated *L* shell. This PSD is a function of frequency *f*, *L*, and *Kp* level, as PSD(*f*, *L*, *Kp*). In this study, we calculate the PSD for *f* from 0.5 to 10 mHz, *L* from 3.5 to 7.5, and *Kp* for the six levels defined earlier, covering the requirement for diffusion coefficient calculation. The PSD(*f*, *L*, *Kp*) array is shown in Figure 2 as functions of frequency in *x* axis for $L = 3.5$ to 7.5 in Figures 2a–2e, respectively. The lines in different colors are plotted for different *Kp* levels as labeled. It is shown that the drift-averaged PSD generally decreases with increasing frequency.

D_{LL}^E is calculated based on equation (1) with the input of PSD(*f*, *L*, *Kp*) array for four μ values of 500, 1000, 2000, and 4000 MeV/G, corresponding roughly to 0.5, 1, 2, and 4 MeV electrons at geosynchronous orbit ($L = 6.6$), respectively. We assume azimuthal mode number $m = 1$ and interpolate PSD(*f*, *L*, *Kp*) along the *f* axis to get PSD(μ, *L*, *Kp*) at the drift frequency of electrons with magnetic moment μ. The D_{LL}^E values are subsequently calculated using equation (1).

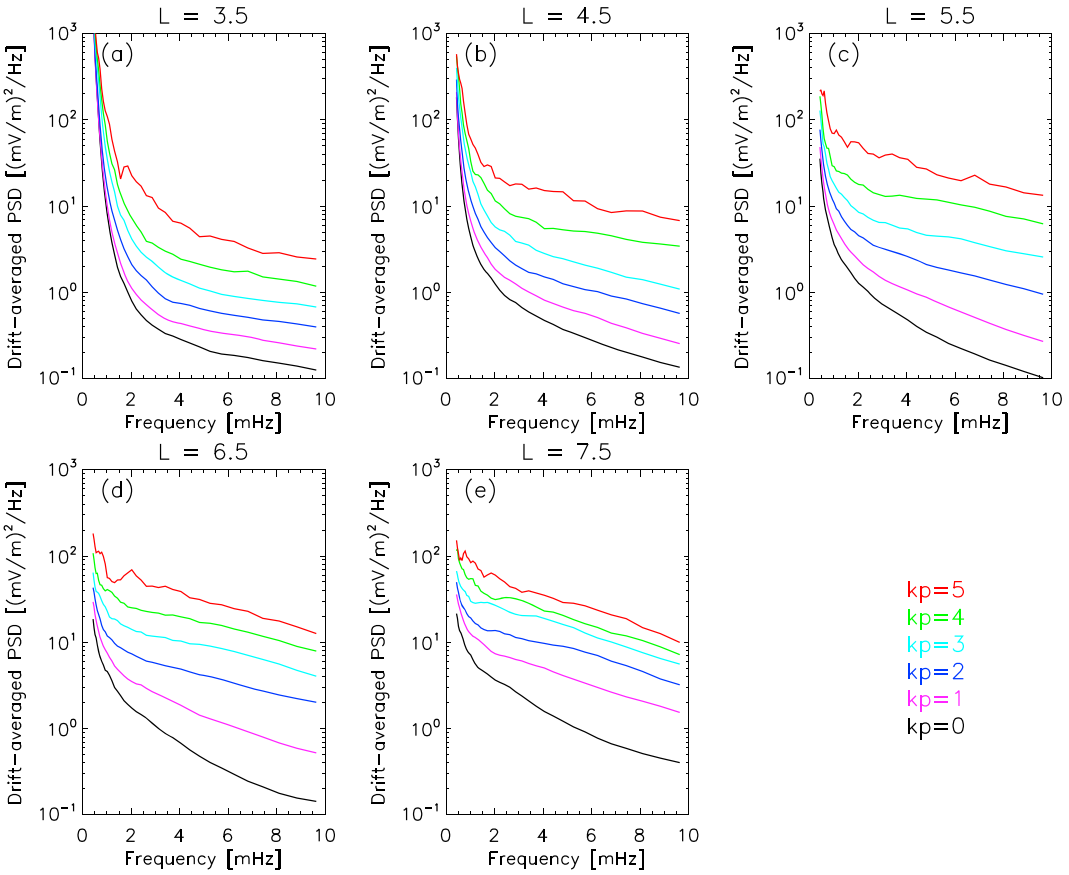

Figure 2. Drift-averaged PSD as functions of frequency for (a–e) $L = 3.5$ to 7.5. Lines in different colors are plotted for different *Kp* levels as labeled.

The calculated D_{LL}^{E}, termed as D_{LL}^{E}[THEMIS], are shown in Figure 3, solid lines, for $\mu = 500$, 1000, 2000, and 4000 MeV/G in Figures 3a–3d, respectively. Lines in different colors are plotted for different *Kp* levels as labeled. It is shown that D_{LL}^{E}[THEMIS] increases with increasing *L* and *Kp* but decreases with increasing μ. Based on the multiparameter linear regression fitting technique, D_{LL}^{E}[THEMIS] can be expressed analytically as

$$D_{LL}^{E}[\text{THEMIS}] = 1.115\cdot10^{-6}\cdot10^{0.281\times Kp}\cdot L^{8.184}\cdot\mu^{-0.608} \quad (2)$$

The fitted D_{LL}^{E}[THEMIS] is plotted as the dashed lines in Figure 3. The correlation coefficient between the original and fitted D_{LL}^{E}[THEMIS] is 0.95. We note here that the root-mean-square errors (RMSE) between the logarithm of the original and fitted coefficient have also been tested for μ values from 100 to 8000 MeV/G. It is found that the RMSE value change slightly at $\mu = 400$–8000 MeV/G but increases dramatically at $\mu < 400$ MeV/G. This indicates that one should be careful when using D_{LL}^{E}[THEMIS] to study the radial diffusion of electrons below 400 MeV/G.

4. Discussion and Conclusions

In Figure 4, for the case of $\mu = 1000$ MeV/G, we compare our D_{LL}^{E}[THEMIS] model, plotted as solid lines, with previous D_{LL} models D_{LL}^{E}[CRRES], D_{LL}^{M}[B-A], and D_{LL}^{E}[Ozeke] models, plotted as dashed lines, dotted lines, and long dashed lines, respectively. The results under quiet geomagnetic activity ($Kp = 1$) and under active geomagnetic activity ($Kp = 5$) are plotted in black and red, respectively.

First, we compare D_{LL}^{E}[THEMIS] (solid lines) with D_{LL}^{E}[CRRES] (dashed lines), which is also based on in situ electric field measurements. We can see that these two models show good consistency in terms of *Kp*

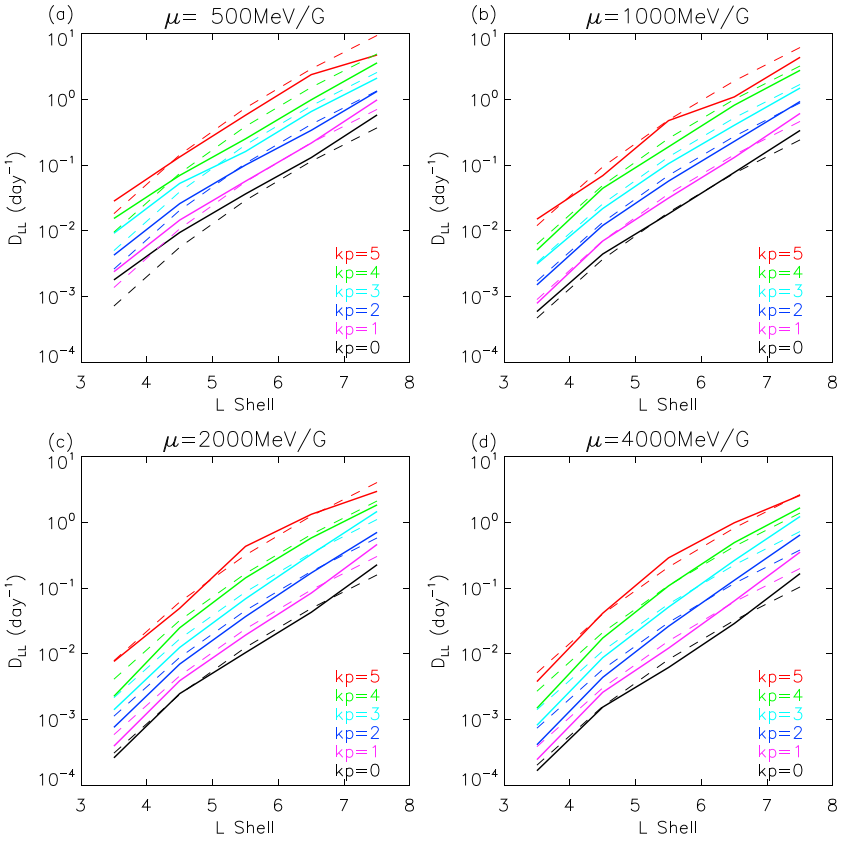

Figure 3. Calculated (solid lines) and fitted (dashed lines) D_{LL}^{E}[THEMIS] plotted as a function of L for (a) $\mu = 500$, (b) $\mu = 1000$, (c) $\mu = 2000$, and (d) $\mu = 4000$ MeV/G. Lines in different colors are plotted for different Kp levels as labeled.

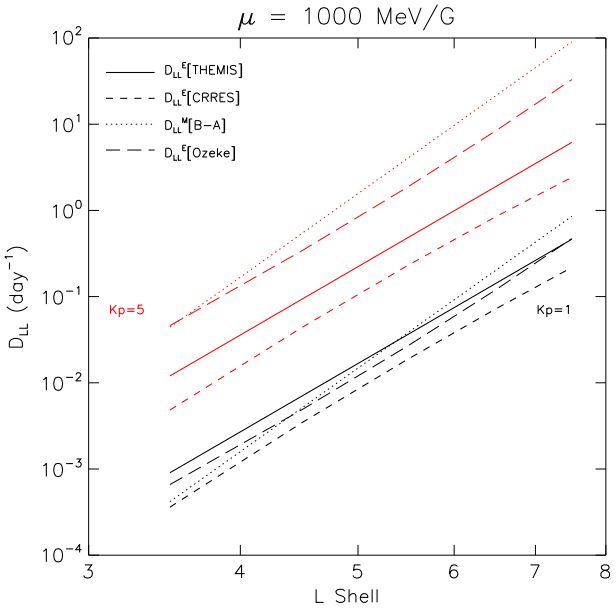

Figure 4. Comparison of D_{LL}^{E}[THEMIS] (solid lines) with other D_{LL} models for the case of $\mu = 1000$ MeV/G and for $Kp = 1$ (in black) and $Kp = 5$ (in red). D_{LL}^{E}[CRRES], D_{LL}^{M}[B-A], and D_{LL}^{E}[Ozeke] are plotted as dashed, dotted, and long dashed lines, respectively.

dependence and L dependence. For example, while Kp value increases from 1 to 5, D_{LL}^{E}[THEMIS] increases by about 1.12 order of magnitude and D_{LL}^{E}[CRRES] increases by about 1.07 order of magnitude. It is also shown that D_{LL}^{E}[THEMIS] is consistently higher than D_{LL}^{E}[CRRES] with roughly a factor of 2. For example, at $L = 6.5$, D_{LL}^{E}[THEMIS] is 0.14 day^{-1} for $Kp = 1$ and 1.90 day^{-1} for $Kp = 5$, while D_{LL}^{E}[CRRES] is 0.07 day^{-1} for $Kp = 1$ and 0.85 day^{-1} for $Kp = 5$. The difference between the absolute values of D_{LL}^{E}[THEMIS] and D_{LL}^{E}[CRRES] could be explained by the orbital coverage of CRRES, which does not cover the high L region in the prenoon sector. As shown in the PSD distributions in Figure 1, this region generally contains high ULF wave power, the missing of which could lead to the underestimation of drift-averaged PSD for calculating D_{LL}^{E}[CRRES]. As mentioned in section 1, CRRES could measure 2-D electric field only in the y and z directions of GSM coordinate system. Thus, additional assumption of $E \cdot B = 0$ is needed to calculate the third component. This assumption is valid only for nontrivial B_x, which substantially reduces the data volume of PSD and prevents any detailed analysis without large database. The same difficulty rises when one uses electric field measurements of Van Allen Probes to calculate the PSD of E_φ. THEMIS satellite measures 2-D electric field near the equatorial plane and thus is a better candidate for the study of equatorial electric field wave power.

Now we compare D_{LL}^{E}[THEMIS] (solid lines) with the other two commonly used D_{LL} models, D_{LL}^{M}[B-A] (dotted lines) and D_{LL}^{E}[Ozeke] (long dashed lines). *Brautigam and Albert* [2000] also calculated $D_{LL}^{E_{static}}$[B-A] containing only the electrostatic radial diffusion coefficient. However, for the L range studied in this paper, their electrostatic diffusion coefficient is generally small and is negligible; thus, we only compare the electromagnetic D_{LL}^{M}[B-A] in this paper. Under quiet geomagnetic conditions, as the black lines shown for $Kp = 1$, the diffusion coefficients of the three models are in the same level. However, the differences in Kp dependence are significant between the models. D_{LL}^{E}[THEMIS] increases by about 1 order of magnitude as Kp value increases from 1 to 5, while the two previous models increase by about 2 orders of magnitudes, i.e., 2.02 orders of magnitude for D_{LL}^{M}[B-A] and 1.84 orders of magnitude for D_{LL}^{E}[Ozeke]. Another difference is the μ dependence (energy dependence) of the diffusion coefficient, which is not included in D_{LL}^{M}[B-A] and D_{LL}^{E}[Ozeke] models. In our model, D_{LL}^{E}[THEMIS] decreases as μ increases as described by a power law index of -0.608. For given frequency range and L range, there will be only a range of energy of electrons that will be drift resonant with the ULF waves. The higher μ electrons may become less resonant with the ULF waves. Also statistically, as shown in Figure 2, the ULF wave PSD almost always decreases with increasing frequency. Electrons with higher energy have higher drift frequency and thus higher resonance frequency. So, in general, less power is available for higher-energy electrons, which is likely another reason why the D_{LL}^{E} decreases as μ increases. For example, at $L = 6.5$, the drift frequencies of electrons in dipole magnetic field of $\mu = 1000$ and 4000 MeV/G are 1.20 and 2.59 mHz, respectively. From the PSD(f, L, Kp) array shown in Figure 2, we can get the PSD of the ULF wave resonant with the electrons, which is 6.09 and 2.97 (mV/m)^2/Hz for the case of $Kp = 1$, i.e., a decrease of ~50% while μ increases from 1000 to 4000 MeV/G. This results in the decrease of calculated D_{LL}^{E}[THEMIS] from 0.13 to 0.06 day^{-1} as μ increases from 1000 to 4000 MeV/G.

The calculation of D_{LL}^{E} in this paper is performed under two assumptions. The first is the assumption of dipole magnetic field model. Under this assumption, one can easily calculate the drift-averaged PSD at each designated L shell. The more accurate calculation of drift-averaged PSD can be made with consideration of compressed magnetic field models, which requires tracing electrons along drift orbits [*Yu et al*., 2014] and also theoretical modification on equation (1). The second assumption is the azimuthal mode number m equal to 1. *Tu et al*. [2012] have made effort on estimating m with MHD simulation, and *Sarris* [2014] estimated m based on multiple GOES measurements. These studies showed while $m = 1$ mode is normally dominant, the power in $m = 2, 3, 4, \ldots$ can be significant and not negligible. However, it is still difficult to systematically determine m number with in situ measurements. Further improvement on D_{LL} will be able to be made once better knowledge of the dependence of PSD on m number is achieved.

The D_{LL}^{E}[THEMIS] calculated in this paper is based on the in situ electric field measurements and contains the diffusion coefficient from both induced and convective electric field. Previous studies [*Tu et al*., 2012; *Ozeke et al*., 2014; *Ali et al*., 2015] have shown that D_{LL}^{B} is much smaller than D_{LL}^{E} by orders of magnitude for the L range studied in the paper. Therefore, one could safely ignore D_{LL}^{B} and use D_{LL}^{E}[THEMIS] as the total D_{LL}.

In summary, based on the long-term in situ measurements on electric field by THEMIS mission, we have obtained the statistical distributions of ULF wave power of E_φ component for different *Kp* levels (Figure 1), which is compelling. The electric radial diffusion coefficient is subsequently calculated based on these distributions. The calculated $D_{LL}^{E}[\mathrm{THEMIS}]$ is fitted as functions of μ, *L*, and *Kp* value. The empirical and convenient form of diffusion coefficient provided in this paper, which also has energy dependence, will be an important contributor to quantify the radial diffusion process of radiation belt electrons.

Acknowledgments
This work is supported by NSFC grants (41274166, 41574154, and 41104109). The work by X. Li was supported by National Science Foundation grant (AGS 1131869). The work by W. Tu was supported by NASA grant (NNX15AW06G). This work receives EU support through the FP7-Space grant agreement 284520 for the MAARBLE collaborative research project. We acknowledge NASA contract NAS5-02099 and V. Angelopoulos for use of data from the THEMIS Mission. Specifically, we acknowledge J.W. Bonnell and F.S. Mozer for use of EFI data. We acknowledge the WDC for Geomagnetism, Kyoto University, Japan, for the geomagnetic indices.

References

Ali, A. F., S. R. Elkington, W. Tu, L. G. Ozeke, A. A. Chan, and R. H. W. Friedel (2015), Magnetic field power spectra and magnetic radial diffusion coefficients using CRRES magnetometer data, *J. Geophys. Res. Space Physics*, *120*, 973–995, doi:10.1002/2014JA020419.

Angelopoulos, V. (2008), The THEMIS mission, *Space Sci. Rev.*, doi:10.1007/s11214-008-9336-1.

Bonnell, J. W., F. S. Mozer, G. T. Delory, A. J. Hull, R. E. Ergun, C. M. Cully, V. Angelopoulos, and P. R. Harvey (2008), The Electric Field Instrument (EFI) for THEMIS, *Space Sci. Rev.*, doi:10.1007/s11214-008-9469-2.

Brautigam, D. H., and J. M. Albert (2000), Radial diffusion analysis of outer radiation belt electrons during October 9, 1990 magnetic storm, *J. Geophys. Res.*, *105*, 291–309, doi:10.1029/1999JA900344.

Brautigam, D. H., G. P. Ginet, J. M. Albert, J. R. Wygant, D. R. Rowl, A. Ling, and J. Bass (2005), CRRES electric field power spectra and radial diffusion coefficients, *J. Geophys. Res.*, *110*, A02214, doi:10.1029/2004JA010612.

Cao, J. B., et al. (2008), Characteristics of mid-low latitude Pi2 excited by bursty bulk flows, *J. Geophys. Res.*, *113*, A07S15, doi:10.1029/2007JA012629.

Cao, J.-B., et al. (2010), Geomagnetic signatures of current wedge produced by fast flows in a plasma sheet, *J. Geophys. Res.*, *115*, A08205, doi:10.1029/2009JA014891.

Dai, L., et al. (2013), Excitation of poloidal standing Alfvén waves through drift resonance wave-particle interaction, *Geophys. Res. Lett.*, *40*, 4127–4132, doi:10.1002/grl.50800.

Dai, L., et al. (2015), Storm time occurrence and spatial distribution of Pc4 poloidal ULF waves in the inner magnetosphere: A Van Allen Probes statistical study, *J. Geophys. Res. Space Physics*, *120*, 4748–4762, doi:10.1002/2015JA021134.

Fälthammar, C.-G. (1965), Effects of time-dependent electric fields on geomagnetically trapped radiation, *J. Geophys. Res.*, *70*, 2503–2516, doi:10.1029/JZ070i011p02503.

Fei, Y., A. A. Chan, S. R. Elkington, and M. J. Wiltberger (2006), Radial diffusion and MHD particle simulations of relativistic electron transport by ULF waves in the September 1998 storm, *J. Geophys. Res.*, *111*, A12209, doi:10.1029/2005JA011211.

Fu, H. S., J. B. Cao, B. Yang, and H. Y. Lu (2011), Electron loss and acceleration during storm time: The contribution of wave-particle interaction, radial diffusion, and transport processes, *J. Geophys. Res.*, *116*, A10210, doi:10.1029/2011JA016672.

Hartinger, M., V. Angelopoulos, M. B. Moldwin, K.-H. Glassmeier, and Y. Nishimura (2011), Global energy transfer during a magnetospheric field line resonance, *Geophys. Res. Lett.*, *38*, L12101, doi:10.1029/2011GL047846.

Huang, C.-L., H. E. Spence, M. K. Hudson, and S. R. Elkington (2010), Modeling radiation belt radial diffusion in ULF wave fields: 2. Estimating rates of radial diffusion using combined MHD and particle codes, *J. Geophys. Res.*, *115*, A06216, doi:10.1029/2009JA014918.

Kepko, L., and M. Kivelson (1999), Generation of Pi2 pulsations by bursty bulk flows, *J. Geophys. Res.*, *104*, 25,021–25,034, doi:10.1029/1999JA900361.

Klimushkin, D. Y., and P. N. Mager (2015), The Alfvén mode gyrokinetic equation in finite-pressure magnetospheric plasma, *J. Geophys. Res. Space Physics*, *120*, 4465–4474, doi:10.1002/2015JA021045.

Lejosne, S., D. Boscher, V. Maget, and G. Rolland (2013), Deriving electromagnetic radial diffusion coefficients of radiation belt equatorial particles for different levels of magnetic activity based on magnetic field measurements at geostationary orbit, *J. Geophys. Res. Space Physics*, *118*, 3147–3156, doi:10.1002/jgra.50361.

Leonovich, A. S., V. V. Mishin, and J. B. Cao (2003), Penetration of magnetosonic waves into the magnetosphere: Influence of a transition layer, *Ann. Geophys.*, *21*(5), 1083–1093.

Li, L., J. B. Cao, and G. C. Zhou (2005), Combined acceleration of electrons by whistler-mode and compressional ULF turbulences near the geosynchronous orbit, *J. Geophys. Res.*, *110*, A03203, doi:10.1029/2004JA010628.

Liu, W., T. E. Sarris, X. Li, S. R. Elkington, R. Ergun, V. Angelopoulos, J. Bonnell, and K. H. Glassmeier (2009), Electric and magnetic field observations of Pc4 and Pc5 pulsations in the inner magnetosphere: A statistical study, *J. Geophys. Res.*, *114*, A12206, doi:10.1029/2009JA014243.

Liu, W., T. E. Sarris, X. Li, R. Ergun, V. Angelopoulos, J. Bonnell, and K. H. Glassmeier (2010), Solar wind influence on Pc4 and Pc5 ULF wave activity in the inner magnetosphere, *J. Geophys. Res.*, *115*, A12201, doi:10.1029/2010JA015299.

Liu, W., J. B. Cao, X. Li, T. E. Sarris, Q.-G. Zong, M. Hartinger, K. Takahashi, H. Zhang, Q. Q. Shi, and V. Angelopoulos (2013), Poloidal ULF wave observed in the plasmasphere boundary layer, *J. Geophys. Res. Space Physics*, *118*, 4298–4307, doi:10.1002/jgra.50427.

Lu, L., Z.-X. Liu, and J.-B. Cao (2002), Two-and-one-half- MHD simulations of the plasma sheet in the presence of oxygen ions: The plasma sheet oscillation and compressional Pc 5 waves, *Phys. Plasmas*, *9*(2), 624–628.

Mcpherron, R. (2005), Magnetic pulsations: Their sources and relation to solar wind and geomagnetic activity, *Surv. Geophys.*, *26*, 545–592, doi:10.1007/s10712-005-1758-7.

Morlet, J., G. Arens, E. Fourgeau, and D. Giard (1982), Wave propagation and sampling theory, *Geophysics*, *47*(2), 203–236.

Ozeke, L. G., I. R. Mann, K. R. Murphy, I. J. Rae, D. K. Milling, S. R. Elkington, A. A. Chan, and H. J. Singer (2012), ULF wave derived radiation belt radial diffusion coefficients, *J. Geophys. Res.*, *117*, A04222, doi:10.1029/2011JA017463.

Ozeke, L. G., I. R. Mann, K. R. Murphy, I. Jonathan Rae, and D. K. Milling (2014), Analytic expressions for ULF wave radiation belt radial diffusion coefficients, *J. Geophys. Res. Space Physics*, *119*, 1587–1605, doi:10.1002/2013JA019204.

Sarris, T. E. (2014), Estimates of the power per mode number of broadband ULF waves at geosynchronous orbit, *J. Geophys. Res. Space Physics*, *119*, 5539–5550, doi:10.1002/2013JA019238.

Sarris, T. E., et al. (2009), Characterization of ULF pulsations by THEMIS, *Geophys. Res. Lett.*, *36*, L04104, doi:10.1029/2008GL036732.

Schulz, M., and L. J. Lanzerotti (1974), *Particle Diffusion in the Radiation Belts*, Springer, New York.

Su, Z., F. Xiao, H. Zheng, and S. Wang (2011), Radiation belt electron dynamics driven by adiabatic transport, radial diffusion, and wave-particle interactions, *J. Geophys. Res.*, *116*, A04205, doi:10.1029/2010JA016228.

Takahashi, K., M. D. Hartinger, V. Angelopoulos, and K.-H. Glassmeier (2015a), A statistical study of fundamental toroidal mode standing Alfvén waves using THEMIS ion bulk velocity data, *J. Geophys. Res. Space Physics*, *120*, 6474–6495, doi:10.1002/2015JA021207.

Takahashi, K., R. E. Denton, W. Kurth, C. Kletzing, J. Wygant, J. Bonnell, L. Dai, K. Min, C. W. Smith, and R. MacDowall (2015b), Externally driven plasmaspheric ULF waves observed by the Van Allen Probes, *J. Geophys. Res. Space Physics*, *120*, 526–552, doi:10.1002/2014JA020373.

Thorne, R. M. (2010), Radiation belt dynamics: The importance of wave-particle interactions, *Geophys. Res. Lett.*, *37*, L22107, doi:10.1029/2010GL044990.

Tu, W., S. R. Elkington, X. Li, W. Liu, and J. Bonnell (2012), Quantifying radial diffusion coefficients of radiation belt electrons based on global MHD simulation and spacecraft measurements, *J. Geophys. Res.*, *117*, A10210, doi:10.1029/2012JA017901.

Xiao, F., Z. Su, H. Zheng, and S. Wang (2009), Modeling of outer radiation belt electrons by multidimensional diffusion process, *J. Geophys. Res.*, *114*, A03201, doi:10.1029/2008JA013580.

Yeoman, T. K., M. James, P. N. Mager, and D. Y. Klimushkin (2012), SuperDARN observations of high-*m* ULF waves with curved phase fronts and their interpretation in terms of transverse resonator theory, *J. Geophys. Res.*, *117*, A06231, doi:10.1029/2012JA017668.

Yu, Y., J. Koller, V. K. Jordanova, S. G. Zaharia, R. W. Friedel, S. K. Morley, Y. Chen, D. Baker, G. D. Reeves, and H. E. Spence (2014), Application and testing of the L* neural network with the self-consistent magnetic field model of RAM-SCB, *J. Geophys. Res. Space Physics*, *119*, 1683–1692, doi:10.1002/2013JA019350.

Zhou, X.-Z., Z.-H. Wang, Q.-G. Zong, S. G. Claudepierre, I. R. Mann, M. G. Kivelson, V. Angelopoulos, Y.-X. Hao, Y.-F. Wang, and Z.-Y. Pu (2015), Imprints of impulse-excited hydromagnetic waves on electrons in the Van Allen radiation belts, *Geophys. Res. Lett.*, *42*, 6199–6204, doi:10.1002/2015GL064988.